Alzheimer's & Dementia: Diagnosis, Assessment & Disease Monitoring 10 (2018) 210-216

Special Section: State of the Field: Advances in Neuroimaging from the 2017 Alzheimer's Imaging Consortium

Elevated medial temporal lobe and pervasive brain tau-PET signal in normal participants

Val J. Lowe[a,*], Tyler J. Bruinsma[a], Hoon-Ki Min[a], Emily S. Lundt[b], Ping Fang[a], Matthew L. Senjem[a,c], Bradley F. Boeve[d], Keith A. Josephs[d], Mukesh K. Pandey[a], Melissa E. Murray[e], Kejal Kantarci[a], David T. Jones[a,d], Christopher G. Schwarz[a], David S. Knopman[d], Ronald C. Petersen[d], Clifford R. Jack, Jr.[a]

[a]*Department of Radiology, Mayo Clinic, Rochester, MN, USA*
[b]*Department of Biomedical Statistics and Informatics, Mayo Clinic, Rochester, MN, USA*
[c]*Department of Information Technology, Mayo Clinic, Rochester, MN, USA*
[d]*Department of Neurology, Mayo Clinic, Rochester, MN, USA*
[e]*Department of Neurology, Mayo Clinic, Jacksonville, FL, USA*

Abstract

Introduction: Medial temporal lobe (MTL) uptake on tau–positron emission tomography (PET) is seen not only in Alzheimer's disease (AD) dementia but also in the aging population. The relationship of these findings to the development of AD dementia needs to be better understood.
Methods: Tau-PET with AV-1451 was performed on 576 cognitively unimpaired (CU) participants aged 50–94 years. The number of CUs with and without abnormal MTL regions and those with or without extra-MTL abnormalities was determined. Left and right regions were compared within each subject.
Results: Of CUs, 58% (334/576) had abnormal tau-PET findings. MTL abnormalities were present in 41% (238/576) of subjects.
Discussion: MTL tau-PET signal is often associated with abnormal extra-MTL tau-PET signal in CU participants and may represent neurofibrillary tangle development that could identify participants most likely to develop AD dementia. Tau-PET signal exclusively outside of the MTL is seen in 17% of CU participants and could be the initial findings in participants in different AD dementia pathways. Significant ($P < .001$) differences in tau–standardized uptake value ratio between sides were noted in 26 of 41 examined brain regions implicating further study of side-specific deficits.

Keywords: Tau-PET; Alzheimer's disease; AV-1451; Imaging; Cognitively normal

1. Introduction

Topographic distribution of neurofibrillary tangles (NFTs) in the brain is the basis for Braak neuropathologic staging of Alzheimer's disease (AD) [1]. Postmortem studies in AD have classified six consecutive Braak stages describing the gradual regional deposition of hyperphosphorylated tau protein over the course of the disease [1,2]. Braak NFT staging is strongly associated with cognitive impairment [1,3–6] and is one of the two hallmark pathological criteria for the diagnosis of AD [7,8]. Braak stage I and stage II are usually clinically asymptomatic with NFT development based in the medial temporal lobe

*Corresponding author. Tel.: +1-507-284-9599, Fax: +1-507-266-4461.
E-mail address: vlowe@mayo.edu

https://doi.org/10.1016/j.dadm.2018.01.005

(MTL) and transentorhinal region in stage I, followed by the entorhinal cortex in stage II. Stage III is marked by the gradual spread of NFT into the limbic structures including the amygdala and hippocampus, with stage IV noting spread to the thalamus and claustrum. Mild clinical symptoms will develop in stages III–IV. The presence of NFTs in the isocortical areas, particularly the neocortical association areas, is indicative of stage V; and stage VI is denoted by severe involvement of all isocortical areas including the primary motor, sensory, and visual areas. The classic clinical phenotype of dementia is evident when stages V–VI are reached [1,5,9,10].

The most confident indication that AD pathology underlies antemortem cognitive impairment corresponds to cases with high densities of amyloid plaques and Braak stages V or VI on postmortem autopsy [11]; however, autopsy results of cognitively unimpaired (CU) individuals show considerable diagnostic overlap with those who are clinically impaired [12]. Autopsy data of NFT pathology in the clinically unimpaired elderly shows that it is largely confined to the entorhinal and adjacent temporal isocortices and not often seen in extratemporal regions [1,13–15]. Postmortem autopsy information is limited to observation of end-stage results and lacks significant observation of how early Braak stage (I and II) would progress to later stage of Braak and whether early-stage Braak is the predecessor of the later stage of Braak that would eventually progress to AD. Furthermore, pathological assessment is necessarily limited to sampling a subset of regions, meaning tau in under-sampled regions may be missed or underreported.

AV-1451 PET imaging and Pittsburgh compound B PET imaging provide a method for study of the progressive pathology of AD in vivo [16–18], and initial studies show that AV-1451 PET can identify AD NFTs [19]. Recent studies have shown that tau-PET closely mimics Braak NFT staging in AD [20–22]. In normal aging, tau-PET signal has been described to occur in the MTL and in pervasive locations colocalized with amyloid deposits [23]. We have recently shown that widespread brain tau can be seen even in the absence of amyloid deposits [24]. Understanding the progressive formation and diffusion of tau before clinical symptoms is an important next step in the earlier diagnosis of AD. In addition, defining tau-PET signal patterns in relation to further development of AD phenotypes is a key to better predict future progression. There is also particular interest regarding early Braak stages (I and II) as potential initial indicators of AD before clinical symptoms. Our goal with the present study is to better understand tau-PET and therefore NFT distribution in CU for future longitudinal studies examining AD pathology development in vivo. We analyzed our results based on early tau-PET abnormalities particularly regarding MTL and extra-MTL regional uptake to understand the frequency of extra-medial tau-PET abnormalities in CU participants.

2. Methods

2.1. Subjects

Participants were part of the Mayo Clinic Study of Aging (MCSA) or Mayo Clinic Alzheimer's Disease Research Center. The MCSA is a randomized, population-based aging study focused on non-demented individuals and encompasses a wide age range [25]. The Mayo Clinic Alzheimer's Disease Research Center is a clinic-based study that reflects the referral patterns of a tertiary academic center. There were 576 CU participants aged 50–94 years who completed tau-PET imaging. The participants were determined to be clinically unimpaired by a MCSA consensus diagnosis (this includes quantitative data as well as clinical and cognitive assessments by neurologists, geriatricians, neuropsychologists, and study coordinators). Apolipoprotein E (*APOE*) status was provided through genetic analysis previously performed in the studies. No adverse events were seen from imaging. All participants or designees provided written consent with approval of Mayo Clinic and Olmsted Medical Center Institutional Review Boards.

2.2. Neuroimaging

For Tau-PET, participants were injected with 370 MBq (range 333–407) of F-18-AV-1451 before imaging and imaging was performed as four, 5-minute frames for a 20-minute PET acquisition, 80–100 minutes post-injection. Amyloid-PET imaging was performed using Pittsburgh compound B and consisted of four 5-minute dynamic frames acquired 40–60 minutes after injection of 628 MBq (range 385 to 723 MBq) of C-11-Pittsburgh compound B as previously described [26]. Magnetic resonance imaging (MRI) scans at 3T with a three-dimensional volumetric T1 magnetization-prepared rapid gradient-echo sequence were performed as previously described [27].

2.3. Image analysis

Cortical regions of interest (ROIs) were defined by an in-house version of the automated anatomic labeling atlas [28] as previously described [29]. Nonlinear registration using SPM5 [30] was used to apply the atlas to each subject's MRI. The static tau-PET and amyloid-PET image volumes of each subject were coregistered to his/her own T1-weighted MRI scan. Statistics on image voxel values from each side of the brain were extracted from each labeled cortical ROI in the atlas. Individual tau-PET ROI median values were normalized to cerebellar crus (bilateral crus, 1–2) to calculate regional standardized uptake value ratios (SUVr). Median values were used to protect ROI central tendency values from being skewed by artifactual voxels. The crus region was selected to provide cerebellar gray matter in relative isolation from cerebrospinal fluid spaces (inferiorly) and to avoid adjacency to parahippocampal, fusiform and lingual gyri, to avoid possible bleed-in signal from tau

pathology. SUVr values were gray matter plus white matter sharpened and were not partial volume corrected. Global cortical amyloid-PET SUVr was computed from a meta-ROI normalized to the cerebellar crus where amyloid-PET positive or negative status was based on a cut point of 1.42 as previously described [31].

2.4. Statistical analysis

Abnormal tau-PET was defined as a region-specific SUVr greater than the 95th percentile in a group of 112 CU, MCSA study participants aged 30–49 years who were amyloid negative. We calculated the percentage of participants with elevated tau-PET for each individual ROI. Participants were then grouped as MTL positive or negative and with or without extra-MTL uptake. The MTL regions included were the entorhinal cortex, parahippocampal gyrus, and hippocampus. All other cortical regions, excluding known off-target sites (vermis, thalamus, caudate, pallidum, and putamen) were considered extra-MTL regions. The left and right hemispheres were evaluated independently. Regions with elevated tau-PET signal were compared to regions described by Braak staging. To assess within-subject differences between the left and right hemispheres, we calculated Student's paired *t*-tests. Differences in demographics features were assessed using linear model analysis of variance or Pearson's chi-squared test with Yates' continuity correction for continuous or categorical features, respectively.

3. Results

Subject characteristics by group with tests of association for age, *APOE*, and amyloid status are available in Table 1 and Table 2. Of note, 58% (334/576) of subjects had abnormal tau-PET findings. MTL abnormalities were present in 41% (238/576) of subjects and showed association with increased age and abnormal amyloid status ($P < .001$) but not *APOE* status. Further grouping reveals a subset of subjects (17%, 96/576) with extra-MTL abnormalities without concurrent MTL abnormalities. Only 16 subjects had abnormalities confined to the MTL. Age and amyloid abnormalities were associated with abnormal tau-PET ($P < .001$), but *APOE* status was not ($P = .606$).

Only 10 subjects had MTL uptake limited to the hippocampus. Of subjects identified as having an MTL abnormality, 58% (138/238) had greater than 10 abnormal areas outside of the MTL (Fig. 1). For the subset of subjects without MTL abnormalities, 67 had greater than one extra-MTL abnormality (Fig. 2). Abnormalities in extra-MTL regions were widespread throughout various areas (Fig. 3). Within-subject comparison of brain regions from the left and right sides with Student's paired *t*-test revealed significant individual variation ($P < .05$) in 30 of the total 42 regions analyzed. Fig. 4 illustrates the results of the hemispheric comparison. By region, subjects having a difference in tau-SUVr between sides greater than ten percent ranged from 0 to 46 subjects with a median of six. The amygdala (21/576, 4%), entorhinal cortex (46/576, 8%), and olfactory center (27/576, 5%) demonstrated particularly high incidence of inter-hemisphere differences in tau-SUVr.

4. Discussion

Determining the distribution of NFT accumulation throughout the lifespan is important to better understand the development of AD pathology and clinical symptoms. In this study, we analyzed tangle distribution within the MTL and in extra-MTL cortical regions for each side of the brain by way of tau-PET and assessed relationships between increased age and abnormal amyloid status among groups having abnormal MTL regions, as well as extra-MTL regions. We highlight three major findings. First, abnormal tau-PET results are very common in CU subjects over the age of 50 years. Second, in a majority of CU subjects, MTL tau-PET signal is associated with extra-MTL tau-PET signal. Finally, a sizeable subset of participants with extra-MTL signal without concurrent MTL findings exists, potentially in contrast with classic past descriptions of AD progression and staging or even normal aging.

Table 1
Characteristics of CU participants having abnormal MTL tau-PET signal and having no abnormal MTL signal

Characteristic	MTL (N = 238)	No MTL (N = 338)	Total (N = 576)	*P* value
Age				<.001
Mean (SD)	75.1 (10.1)	68.3 (10.1)	71.1 (10.6)	
Median (Q1, Q3)	76.6 (67.5, 82.6)	67.5 (59.7, 74.9)	70.3 (63.3, 79.5)	
Range	50.5–98.6	50.2–94.9	50.2–98.6	
APOE status				.457
N-missing	8	20	28	
Negative	161 (70%)	233 (73.3%)	394 (71.9%)	
Positive	69 (30%)	85 (26.7%)	154 (28.1%)	
Aβ status				<.001
Negative	119 (50%)	256 (75.7%)	375 (65.1%)	
Positive	119 (50%)	82 (24.3%)	201 (34.9%)	

Abbreviations: CU, cognitively unimpaired; MTL, medial temporal lobe; PET, positron emission tomography; SD, standard deviation; Q1, first quartile; Q3, third quartile; Aβ, amyloid β; APOE, apolipoprotein E.

Table 2
Characteristics of CU participants having abnormal tau-PET signal in MTL and extra-MTL regions

Characteristics	MTL, +1 other (N = 222)	MTL, no others (N = 16)	No MTL, +1 other (N = 96)	No MTL, no others (N = 242)	Total (N = 576)	*P* value
Age						<.001
Mean (SD)	75.1 (10.1)	74.8 (11.3)	69.6 (10.2)	67.8 (10.1)	71.1 (10.6)	
Q1, Q3	67.8, 82.4	66, 86.5	62.5, 77.1	59.2, 73.2	63.3, 79.5	
Range	50.5–98.6	55.9–89.9	51.1–90.6	50.2–94.9	50.2–98.6	
APOE status						.606
N-missing	8	0	3	17	28	
Negative	150 (70.1%)	11 (68.8%)	72 (77.4%)	161 (71.6%)	394 (71.9%)	
Positive	64 (29.9%)	5 (31.2%)	21 (22.6%)	64 (28.4%)	154 (28.1%)	
Aβ status						<.001
Negative	112 (50.5%)	7 (43.8%)	66 (68.8%)	190 (78.5%)	375 (65.1%)	
Positive	110 (49.5%)	9 (56.2%)	30 (31.2%)	52 (21.5%)	201 (34.9%)	

Abbreviations: CU, cognitively unimpaired; PET, positron emission tomography; MTL, medial temporal lobe; SD, standard deviation; Q1, first quartile; Q3, third quartile; Aβ, amyloid β; APOE, apolipoprotein E.

Over half of the studied CU subjects had abnormal tau-PET results. Generally, these abnormal results were significantly associated with advanced age and amyloid accumulation. In other studies, age was not associated with tau-PET signal [20,32]. Our observation of a majority of participants (69%, 66/96) with normal amyloid scans but distributed focal extra-MTL tau-PET signal without abnormal MTL signal contrasts recent findings that tau-PET signal is not found outside of the MTL in amyloid-negative CU older adults (n = 58) [33]. Our image analysis methodology used CU individuals younger than 50 years as a normal baseline and defined abnormalities in each brain region rather than using a meta-ROI or large brain region. We also evaluated the relationship of right- and left-brain tau-PET signal. This is distinct from prior studies that used combined multiregion composite regions, typically intended to mimic Braak stage regional anatomy [20,22,23].

Our results indicate that NFTs as seen by tau-PET in CU individuals can be frequently noted in both the MTL and in the extra-MTL cortex even when MTL abnormalities are absent. Small-cohort autopsy studies support these PET findings demonstrating advanced tangle stages (IV–VI) in clinically impaired and CU subjects [12], "less frequent" but existent isocortical tangles in CU brains [1,14], and variability in pathology leading to small numbers of CU and AD patients presenting with the described Braak NFT hierarchy [34]. Collectively, these autopsy data support less frequent but present NFTs in CU populations, consistent with our tau-PET discoveries.

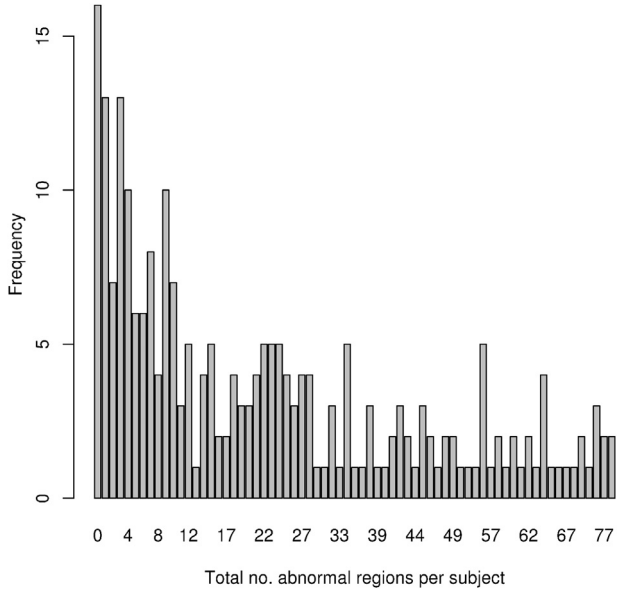

Fig. 1. Bar chart depicting the frequency of extra-MTL tau-PET signal in CN subjects with MTL tau-PET abnormalities. Abbreviations: MTL, medial temporal lobe; CN, cognitively normal.

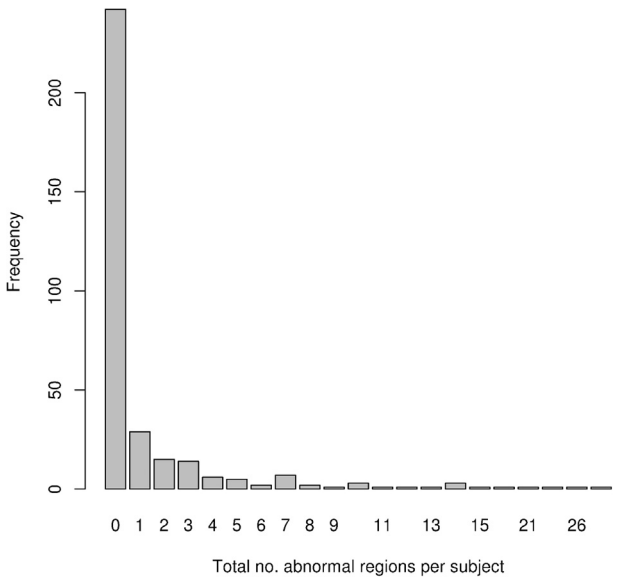

Fig. 2. Bar chart depicting the frequency of extra-MTL tau-PET signal in CN subjects without MTL tau-PET abnormalities. Abbreviations: MTL, medial temporal lobe; CN, cognitively normal.

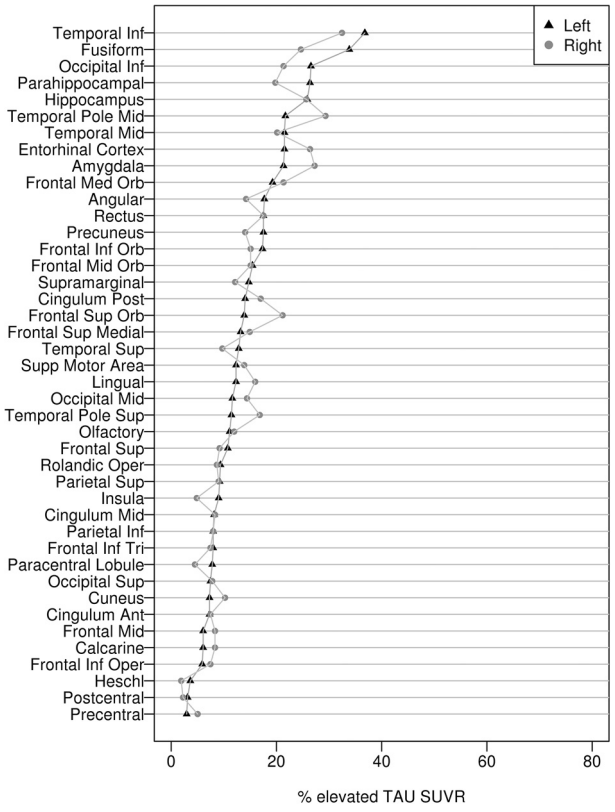

Fig. 3. Percent of tau-PET SUVr values above normal divided by brain region and sorted top to bottom by highest percent in the left hemisphere. Abbreviation: SUVr, standardized uptake value ratios.

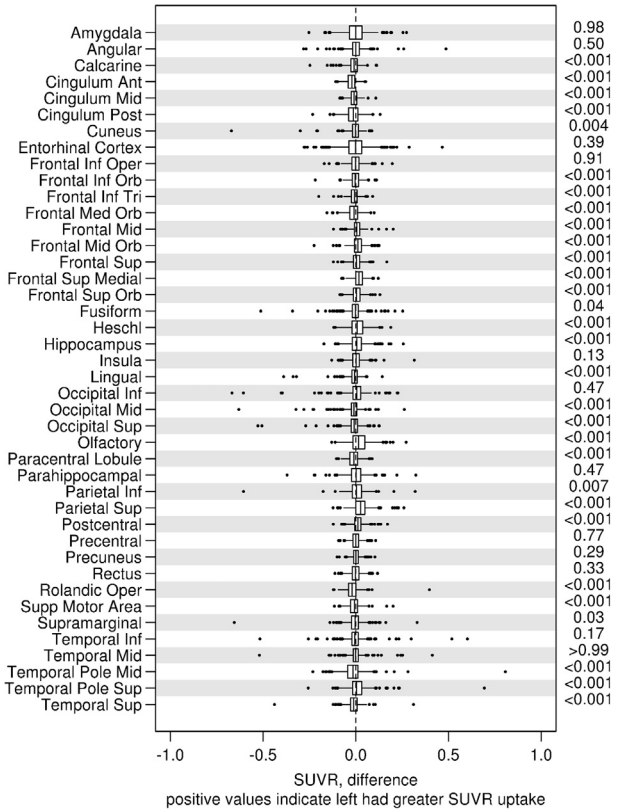

Fig. 4. Tau-SUVr within-subject differences between the left and right hemispheres separated into brain regions. Positive values indicate that the left hemisphere had greater SUVr uptake. Statistical analysis by Student's paired *t*-test reveals statistically significant differences between the left and right sides in 26 regions. Abbreviation: SUVr, standardized uptake value ratios.

In the CU population we studied, MTL tau-PET signal is almost always associated with extra-MTL tau-PET signal supporting Braak staging of more advanced NFT distributions but in a CU population [1]. The subset of CU subjects without MTL tau-PET signal who had extra-MTL uptake (n = 96), however, represent a previously under-reported group. Without notable MTL signal, this group appears to defy traditional Braak staging and therefore could represent an atypical pathology in the AD dementia pathway. Spread-through network connections could induce the distal deposition of tau within a functional network [35]. Observed tau propagation in response to soluble phosphorylated high molecular weight tau in the extracellular space could also contribute to the observed distal spread [36]. Widespread tau proliferation through these mechanisms could provide the backbone for further tangle development in conjunction with amyloid β in disease-related sites. Further longitudinal study of these participants is necessary to better understand the observed anomaly and how it may contribute to the development of AD.

The observed extra-MTL tau-PET abnormalities were typically widespread with multiple areas of uptake noted in most subjects. Though artifact-related tracer activity may be to blame for some cases of extra-MTL, 58% (138/238) of cases with MTL abnormalities have greater than 10 abnormal extra-MTL areas (Fig. 1). In the group with no MTL abnormalities but at least one extra-MTL finding, 70% (67/96) have two or greater areas of elevated tau-PET signal. The frequency of regions with elevated signal and the intensity of the signal (SUVr) indicate that, regardless of cutoff point chosen, significant extra-MTL uptake of tau-PET is evident in CU subjects. We did not correct for multiple comparisons in non-MTL regions as this is an observational study, and we did not want to strongly control the rate of false-positive findings at the expense of false negatives [37]. Many participants with multiple positive non-MTL regions (>4) suggest that the findings of widespread brain tau signal are compelling. This observation needs to be confirmed by others and tested in longitudinal series.

Hemispheric analysis within subjects revealed significant variation ($P < .05$) between the left and right hemispheres in 30 of 42 brain regions. Individual variation of tau deposition between the sides of the brain is an area of interest particularly for explaining side-specific deficits in cognition and neuromotor control. Although average difference between sides in the entire group was 0.03 or less, individual subjects noted much greater SUVr differences particularly in the amygdala, entorhinal cortex,

and olfactory center indicating a potential for clinically relevant variances in individual subjects (Fig. 4). Future work should consider closer examination of side-specific analysis and correlation to clinical presentations on serial follow-up.

Off-target binding presents a potential confounding variable for this study; however, certain measures were put into place to limit the effect of off-target binding on overall results. While AV-1451 tau-PET is relatively specific for AD NFT, we have reported postmortem autoradiography studies demonstrating minimal signal in off-target binding sites [38]. Regions known to have significant off-target uptake such as the putamen were excluded from the extra-MTL groupings. Off-target binding in the choroid plexus could bias MTL findings in regions such as the hippocampus that are proximal to the choroid plexus. Only 10 subjects noted MTL binding limited to just the hippocampus. This could indicate that choroid plexus binding had limited effect on overall study findings. This said, comprehensive analysis of off-target binding of AV-1451 in tau-PET is still being performed. We selected a group of participants younger than 50 years of age to determine "normal" tau-PET signal. Early tau deposition may be present in some of these individuals potentially biasing our results. Autopsy data correlated with in vivo imaging coupled with longitudinal studies is needed to verify age-related increases in tau-PET and relevant clinical implications. Exhaustive analysis is necessary to determine appropriate "disease" cutoffs in tau-PET adjusted for normal pathologies of aging. These findings of tau-PET signal as a representation of tau accumulation in the brain need to be confirmed with more research such as binding correlation studies in tissue, biodistribution studies, and autopsy data correlated with in vivo imaging coupled with longitudinal studies. These data are needed to verify tau binding specificity of tau-PET radiotracers, age-related increases in tau-PET, and any relevant clinical correlations and implications.

Acknowledgments

The authors would like to greatly thank AVID Radiopharmaceuticals, Inc., for their support in supplying AV-1451 precursor, reference standards, and FDA regulatory cross-filing permission and documentation needed for this work.

This research was supported by NIH grants, P50 AG016574, R01 NS89757, R01 NS089544, R01 DC10367, U01 AG006786, R21 NS094489, R01 AG 011378, R01 AG 041851, the Robert Wood Johnson Foundation, The Elsie and Marvin Dekelboum Family Foundation, The Liston Family Foundation, the Robert H. and Clarice Smith and Abigail van Buren Alzheimer's Disease Research Program, The GHR Foundation, Foundation Dr. Corinne Schuler, and the Mayo Foundation.

RESEARCH IN CONTEXT

1. Systematic review: The authors reviewed the literature using traditional sources and meeting abstracts and presentations. Exhaustive characterization of AV-1451 in both Alzheimer's disease (AD) and cognitively normal cases is currently in process, and several recent publications have described aspects of the tracer in AD patients and small cohorts of cognitively normal patients.
2. Interpretation: Our results characterize AV-1451 in a large cognitively normal cohort and report both expected and unexpected findings regarding the intersection of tau-PET imaging and traditional Braak staging of AD.
3. Future directions: Longitudinal studies with autopsy and tau-PET imaging are necessary to better elucidate the pathophysiological development of AD. Further image analysis is also necessary to determine adequate cutoff points for clinical use of AV-1451 as a diagnostic tool.

References

[1] Braak H, Braak E. Neuropathological stageing of Alzheimer-related changes. Acta Neuropathol 1991;82:239–59.
[2] Braak H, Alafuzoff I, Arzberger T, Kretzschmar H, Del Tredici K. Staging of Alzheimer disease-associated neurofibrillary pathology using paraffin sections and immunocytochemistry. Acta Neuropathol 2006;112:389–404.
[3] Bennett DA, Schneider JA, Wilson RS, Bienias JL, Arnold SE. Neurofibrillary tangles mediate the association of amyloid load with clinical Alzheimer disease and level of cognitive function. Arch Neurol 2004; 61:378–84.
[4] Duyckaerts C, Bennecib M, Grignon Y, Uchihara T, He Y, Piette F, et al. Modeling the relation between neurofibrillary tangles and intellectual status. Neurobiol Aging 1997;18:267–73.
[5] Nelson PT, Alafuzoff I, Bigio EH, Bouras C, Braak H, Cairns NJ, et al. Correlation of Alzheimer disease neuropathologic changes with cognitive status: a review of the literature. J Neuropathol Exp Neurol 2012; 71:362–81.
[6] Sabbagh MN, Cooper K, DeLange J, Stoehr JD, Thind K, Lahti T, et al. Functional, global and cognitive decline correlates to accumulation of Alzheimer's pathology in MCI and AD. Curr Alzheimer Res 2010; 7:280–6.
[7] Hyman BT, Phelps CH, Beach TG, Bigio EH, Cairns NJ, Carrillo MC, et al. National Institute on Aging-Alzheimer's Association guidelines for the neuropathologic assessment of Alzheimer's disease. Alzheimers Dement 2012;8:1–13.
[8] Montine TJ, Phelps CH, Beach TG, Bigio EH, Cairns NJ, Dickson DW, et al. National Institute on Aging-Alzheimer's Association guidelines for the neuropathologic assessment of Alzheimer's disease: a practical approach. Acta Neuropathol 2012;123:1–11.

[9] Serrano-Pozo A, Frosch MP, Masliah E, Hyman BT. Neuropathological alterations in Alzheimer disease. Cold Spring Harb Perspect Med 2011;1:a006189.
[10] Riley KP, Snowdon DA, Markesbery WR. Alzheimer's neurofibrillary pathology and the spectrum of cognitive function: findings from the Nun Study. Ann Neurol 2002;51:567–77.
[11] Abner EL, Kryscio RJ, Schmitt FA, Santacruz KS, Jicha GA, Lin Y, et al. "End-stage" neurofibrillary tangle pathology in preclinical Alzheimer's disease: fact or fiction? J Alzheimers Dis 2011;25:445–53.
[12] Gertz HJ, Xuereb JH, Huppert FA, Brayne C, Kruger H, McGee MA, et al. The relationship between clinical dementia and neuropathological staging (Braak) in a very elderly community sample. Eur Arch Psychiatry Clin Neurosci 1996;246:132–6.
[13] Braak H, Braak E. Frequency of stages of Alzheimer-related lesions in different age categories. Neurobiol Aging 1997;18:351–7.
[14] Arriagada PV, Marzloff K, Hyman BT. Distribution of Alzheimer-type pathologic changes in nondemented elderly individuals matches the pattern in Alzheimer's disease. Neurology 1992;42:1681–8.
[15] Bouras C, Hof PR, Giannakopoulos P, Michel JP, Morrison JH. Regional distribution of neurofibrillary tangles and senile plaques in the cerebral cortex of elderly patients: a quantitative evaluation of a one-year autopsy population from a geriatric hospital. Cereb Cortex 1994;4:138–50.
[16] Zimmer ER, Leuzy A, Gauthier S, Rosa-Neto P. Developments in tau PET imaging. Can J Neurol Sci 2014;41:547–53.
[17] Hashimoto H, Kawamura K, Igarashi N, Takei M, Fujishiro T, Aihara Y, et al. Radiosynthesis, photoisomerization, biodistribution, and metabolite analysis of 11C-PBB3 as a clinically useful PET probe for imaging of tau pathology. J Nucl Med 2014;55:1532–8.
[18] Fawaz MV, Brooks AF, Rodnick ME, Carpenter GM, Shao X, Desmond TJ, et al. High affinity radiopharmaceuticals based upon lansoprazole for PET imaging of aggregated tau in Alzheimer's disease and progressive supranuclear palsy: synthesis, preclinical evaluation, and lead selection. ACS Chem Neurosci 2014;5:718–30.
[19] Xia CF, Arteaga J, Chen G, Gangadharmath U, Gomez LF, Kasi D, et al. [(18)F]T807, a novel tau positron emission tomography imaging agent for Alzheimer's disease. Alzheimers Dement 2013;9:666–76.
[20] Schwarz AJ, Yu P, Miller BB, Shcherbinin S, Dickson J, Navitsky M, et al. Regional profiles of the candidate tau PET ligand 18F-AV-1451 recapitulate key features of Braak histopathological stages. Brain 2016;139:1539–50.
[21] Ossenkoppele R, Schonhaut DR, Scholl M, Lockhart SN, Ayakta N, Baker SL, et al. Tau PET patterns mirror clinical and neuroanatomical variability in Alzheimer's disease. Brain 2016;139:1551–67.
[22] Johnson KA, Schultz A, Betensky RA, Becker JA, Sepulcre J, Rentz D, et al. Tau positron emission tomographic imaging in aging and early Alzheimer disease. Ann Neurol 2016;79:110–9.
[23] Scholl M, Lockhart SN, Schonhaut DR, O'Neil JP, Janabi M, Ossenkoppele R, et al. PET imaging of tau deposition in the aging human brain. Neuron 2016;89:971–82.
[24] Lowe VJ, Wiste HJ, Senjem ML, Weigand SD, Therneau TM, Boeve BF, et al. Widespread brain tau and its association with ageing, Braak stage and Alzheimer's dementia. Brain 2018;141:271–87.
[25] Roberts RO, Geda YE, Knopman DS, Cha RH, Pankratz VS, Boeve BF, et al. The Mayo Clinic Study of Aging: design and sampling, participation, baseline measures and sample characteristics. Neuroepidemiology 2008;30:58–69.
[26] Lowe VJ, Weigand SD, Senjem ML, Vemuri P, Jordan L, Kantarci K, et al. Association of hypometabolism and amyloid levels in aging, normal subjects. Neurology 2014;82:1959–67.
[27] Jack CR Jr, Wiste HJ, Knopman DS, Vemuri P, Mielke MM, Weigand SD, et al. Rates of beta-amyloid accumulation are independent of hippocampal neurodegeneration. Neurology 2014;82:1605–12.
[28] Tzourio-Mazoyer N, Landeau B, Papathanassiou D, Crivello F, Etard O, Delcroix N, et al. Automated anatomical labeling of activations in SPM using a macroscopic anatomical parcellation of the MNI MRI single-subject brain. NeuroImage 2002;15:273–89.
[29] Vemuri P, Gunter JL, Senjem ML, Whitwell JL, Kantarci K, Knopman DS, et al. Alzheimer's disease diagnosis in individual subjects using structural MR images: validation studies. NeuroImage 2008;39:1186–97.
[30] Ashburner J, Friston KJ. Unified segmentation. NeuroImage 2005;26:839–51.
[31] Jack CR Jr, Wiste HJ, Weigand SD, Therneau TM, Lowe VJ, Knopman DS, et al. Defining imaging biomarker cut points for brain aging and Alzheimer's disease. Alzheimers Dement 2017;13:205–16.
[32] Brier MR, Gordon B, Friedrichsen K, McCarthy J, Stern A, Christensen J, et al. Tau and Abeta imaging, CSF measures, and cognition in Alzheimer's disease. Sci Transl Med 2016;8:338ra66.
[33] Pontecorvo MJ, Devous MD Sr, Navitsky M, Lu M, Salloway S, Schaerf FW, et al. Relationships between flortaucipir PET tau binding and amyloid burden, clinical diagnosis, age and cognition. Brain 2017;140:748–63.
[34] Gertz HJ, Xuereb J, Huppert F, Brayne C, McGee MA, Paykel E, et al. Examination of the validity of the hierarchical model of neuropathological staging in normal aging and Alzheimer's disease. Acta Neuropathol 1998;95:154–8.
[35] Stancu IC, Vasconcelos B, Ris L, Wang P, Villers A, Peeraer E, et al. Templated misfolding of Tau by prion-like seeding along neuronal connections impairs neuronal network function and associated behavioral outcomes in Tau transgenic mice. Acta Neuropathol 2015;129:875–94.
[36] Takeda S, Wegmann S, Cho H, DeVos SL, Commins C, Roe AD, et al. Neuronal uptake and propagation of a rare phosphorylated high-molecular-weight tau derived from Alzheimer's disease brain. Nat Commun 2015;6:8490.
[37] Rothman KJ. No adjustments are needed for multiple comparisons. Epidemiology 1990;1:43–6.
[38] Lowe VJ, Curran G, Fang P, Liesinger AM, Josephs KA, Parisi JE, et al. An autoradiographic evaluation of AV-1451 Tau PET in dementia. Acta Neuropathol Commun 2016;4:58.